European Review for Medical and Pharmacological Sciences 2020; 24: 2491-2504

LINC00114 promoted nasopharyngeal carcinoma progression and radioresistance *in vitro* and *in vivo* through regulating ERK/JNK signaling pathway *via* targeting miR-203

Y.-Y. HAN[1], K. LIU[2], J. XIE[1], F. LI[1], Y. WANG[1], B. YAN[3]

[1]Department of Otolaryngology Head and Neck Surgery, Urumqi Eye and ENT Specialist Hospital, Urumqi, Xinjiang, China
[2]Department of Head and Neck Radiotherapy, Affiliated Cancer Hospital of Xinjiang Medical University, Urumqi, Xinjiang, China
[3]Department of Ophthalmology and Otorhinolaryngology, Urumqi First People's Hospital, Urumqi, Xinjiang, China

Yanyan Han and *Kai Liu* contributed equally to this work

Abstract. – OBJECTIVE: Nasopharyngeal carcinoma (NPC) is a malignancy and is prone to distant metastasis and radioresistance. Long non-coding RNAs (lncRNAs) play vital roles in human cancers. The purpose of this study was to explore the role and the action mechanism of intergenic lncRNA (LINC00114) in NPC.

MATERIALS AND METHODS: The expression of LINC00114 and microRNA-203 (miR-203) was measured by quantitative real-time polymerase chain reaction (qRT-PCR). NPC cells were exposed to X-ray as radiation treatment. Cell proliferation, migration, cell survival fraction and apoptosis were assessed by 3-(4, 5-dimethyl-2-thiazolyl)-2,5-diphenyl-2-H-tetrazolium bromide (MTT), transwell, colony formation, and flow cytometry assays, respectively. The expression of Cleaved-cas-3, Cleaved-cas-9, phosphor-ERK (p-ERK) and phosphor-JNK (p-JNK) was quantified by Western blot. The interaction between miR-203 and LINC00114 was predicted by bioinformatics tool microRNA.org and verified by dual-luciferase reporter assay. Tumor formation assay in nude mice was conducted to examine the role of LINC00114 *in vivo*.

RESULTS: LINC00114 was upregulated in serums from NPC patients, tissues and cell lines of NPC. LINC00114 knockdown inhibited proliferation, migration, and radioresistance of NPC cells. MiR-203 was a target of LINC00114, and miR-203 inhibition eliminated the effects of LINC00114 knockdown. Besides, the extracellular signal-regulated kinases (ERK)/c-Jun N-terminal kinases (JNK) pathway was inactivated by LINC00114 knockdown but recovered by miR-203 inhibition. Moreover, LINC00114 knockdown suppressed tumor growth and radioresistance *in vivo*.

CONCLUSIONS: LINC00114 contributed to NPC development and radioresistance through the regulation of ERK/JNK signaling pathway and the mediation of miR-203, suggesting that LINC00114 was a promising biomarker to defense NPC progression and radioresistance.

Key Words:
LINC00114, MiR-203, Nasopharyngeal carcinoma, Radioresistance, ERK, JNK.

Introduction

Nasopharyngeal carcinoma (NPC) is a universal head and neck malignancy that derives from the nasopharyngeal epithelium[1]. NPC is not a common tumor worldwide and it has a low incidence[2]. NPC is related to ethnicity and geographic distribution-specific cancer[3] and frequently occurs in southern China, Southeast Asia, and North Africa[4]. The combination of radiotherapy and chemotherapy is an effective treatment for NPC, and most NPC patients at the early stage have been effectively cured due to the improvement of diagnostic techniques and therapies[5]. However, the survival rate within five years of the NPC patients at the advanced stage is unsatisfactory because of drug resistance, radioresistance, distant metastases and localized regional recurrence[6-9]. Therefore, it is necessary to explore novel molecular mechanisms and targets to counter the progression and radioresistance of NPC.

Corresponding Author: Bin Yan, MD; e-mail: xvkzel@163.com

More and more functions of long non-coding RNAs (lncRNAs) have been concerned and explored, such as chromatin modification, transcriptional regulation, and post-transcriptional regulation[10]. LncRNAs are a class of > 200 nucleotides RNA molecules with no or limited protein-coding capacity[10]. The involvement of lncRNAs in the development of human cancers has been widely reported, including that in NPC. Besides, lncRNA AFAP1-AS1 contributed to NPC migration and invasion by activating Rho/Rac pathway *via* targeting miR-423-5p[11]. LncRNA DANCR could enhance the expression of HIF-1α through combining with NF90/NF45 complex, resulting in the progression of HPC[12]. LncRNA FAM225A facilitated the occurrence and metastasis of NPC by acting as a competing endogenous RNA (ceRNA) of miR-590-3p and miR-1275 to increase the abundance of ITGB3[13]. These findings indicated the implication of several lncRNAs in NPC. Intergenic lncRNAs (lincRNAs) originate from the region between two protein-coding genes[14]. LINC00114 is one of the lincRNAs that maps on chr21. It was previously identified between low metastatic NPC cells and high metastatic NPC cells by microarray expression profiling[15]. However, the potential role of LINC00114 in NPC has not been investigated yet.

MicroRNAs (miRNAs) are small non-coding RNAs with about 22 nucleotides[16]. MiRNAs take part in a majority of biological processes through interacting with the 3' untranslated region (3' UTR) of target message RNAs (mRNAs), which is regarded as the canonical action mechanism[17]. Likewise, the involvement of miRNAs in the development of human cancers attracts widespread attention. In NPC, dozens of miRNAs had been reported to be associated with the progression, such as EBV-miR-BART8-3p, miR-9 and miR-506[18-20]. Among these miRNAs, miR-203 was distinguished as a tumor inhibitor with diverse functions in human cancers, including ovarian cancer, prostate cancer and breast cancer[21-23]. Unfortunately, the function of miR-203 in NPC is inadequate, and the related mechanism is lacking. Hence, the role of miR-203 and associated action mechanism were investigated in this paper.

In the present study, the expression analysis of LINC00114 was performed in NPC tissues and cells. The endogenous level of LINC00114 was knocked down to determine its potential role. Besides, the target miRNAs of LINC00114 were identified. The purpose of this study was to figure out the role of LINC00114 and underlying mechanism in the development and radioresistance of NPC.

Materials and Methods

Collection of Serums and Tissues

Patients and volunteers were recruited from Urumqi Eye and ENT Specialist Hospital, and a total of 70 serum specimens from NPC patients, 50 serum specimens from healthy volunteers, 70 paired cancer tissues and adjacent normal tissues were collected. NPC tissues were divided into 2 groups according to the tumor-node-metastasis (TNM) stage, including advanced stage (III and IV) and early stage (I and II). Serum specimens were isolated from blood samples after centrifugation at 2,000 × g for 10 min. All serums and tissues were frozen in liquid nitrogen and stored at -80°C condition. Informed consent was obtained from each subject. This research was authorized by the Ethics Committee of Urumqi Eye and ENT Specialist Hospital.

Cell Lines

NPC cell lines (5-8F and SUNE-1) and human nasopharyngeal epithelium cells (NP69) were purchased from Tongwei Biotechnology (Shanghai, China). All cells were maintained in 90% Roswell Park Memorial Institute-1640 (RPMI 1640; Sigma-Aldrich, St. Louis, MO, USA) containing 10% fetal bovine serum (FBS; Sigma-Aldrich) at 37°C condition with 5% CO_2.

Cell Transfection

Small interference RNA against LINC00114 (si-LINC00114) and its negative control (si-NC) were assembled by Genepharma (Shanghai, China). MiR-203 mimic (miR-203), miR-203 inhibitor (anti-miR-203), and their corresponding controls (miR-NC and anti-NC) were obtained from Ribobio (Guangzhou, China). Lentiviral vector (lenti-short hairpin sh-LINC00114) and its negative control (sh-NC) were obtained from Genechem (Shanghai, China). Cell transfection was carried out in 5-8F and SUNE-1 cells using Lipofectamine 2000 (Invitrogen, Carlsbad, CA, USA). Following experiments were conducted at 48 h post-transfection.

Cell Treatment with Radiation

5-8F and SUNE-1 cells with different transfection were exposed in X-ray radiation at a dose of 0, 2, 4, 6 or 8 Gy at room temperature.

Quantitative Real-Time Polymerase Chain Reaction (qRT-PCR)

Total RNA was separated from NPC tissues and cells using Total RNA Extractor (Sangon Biotech, Shanghai, China). Then, the HiScript III 1st Strand cDNA Synthesis Kit (Vazyme, Nanjing, China) or miRNA 1st Strand cDNA Synthesis Kit (Vazyme) was used to synthesize complementary DNA (cDNA) for LINC00114 or miR-203. Next, qRT-PCR was conducted using SYBR qPCR Master Mix (Vazyme) on a CFX96 touch q-PCR system (Bio-Rad, Hercules, CA, USA). The relative expression was calculated using the $2^{-\Delta\Delta Ct}$ method and normalized by glyceraldehyde-3-phosphate dehydrogenase (GAPDH) or small nuclear RNA U6. All primers were listed as follows: LINC00114, forward (F): 5'-CAATATACCTACAGTTTCCTGGGC-3' and reverse (R): 5'-CATATCTGGAAATGGCCCAGG-3'; GAPDH, F: 5'-CCATGAGAAGTATGACAACAGC-3' and R: 5'-ATGGACTGTGGTCATGAGTC-3'; miR-203, F: 5'-GGGGTGAAATGTTTAGGAC-3' and R: 5'-CAGTGCGTGTCGTGGAGT-3'; U6, F: 5'-GCUUCGGCAGCACAUAUACUAAAAU-3' and R: 5'-CGCUUCACGAAUUUGCGUGUCAU-3'.

3-(4,5-Dimethyl-2-Thiazolyl)-2,5-Diphenyl-2-H-Tetrazolium Bromide (MTT) Assay

To assess cell proliferation, 5-8F and SUNE-1 cells with different transfection were plated into 96-well plates at a density of 5×10^3 cells per well. Then 10 μL MTT solution (Beyotime, Shanghai, China) was added into each well at the indicated time points (0 h, 24 h, 48 h and 72 h) for another 4 h at 37°C. Afterwards, 100 μL dimethyl sulfoxide (DMSO; Beyotime) was pipetted into each well to dissolve the formazan for another 10 min. The optic density (OD) value was detected at 490 nm under a microplate reader (Bio-Rad, Hercules, CA, USA).

Transwell Assay

The 6-well transwell chambers (BD Biosciences, Franklin Lakes, NJ, USA) were adapted to observe cell migration. Briefly, 5-8F and SUNE-1 cells (1×10^5 cells/mL) in fresh Dulbecco's Modified Eagle's Medium (DMEM) containing 10% FBS were placed into the top of chambers. Meanwhile, DMEM containing 10% FBS was added into the bottom of chambers. After reaction for 24 h, the migrated cells in the lower surface were fixed with formaldehyde and stained with 5% crystal violet (Beyotime). The cells were counted using a microscope (Olympus, Tokyo, Japan).

Colony Formation Assay

To monitor the effects of radiation on cell survival, 5-8F and SUNE-1 cells with different transfection were exposed to different doses of radiation with a dose rate of 200 cGy/min. Afterwards, cells were collected into 12-well plates (300 cells/well) and cultured for 10 days. Subsequently, treated cells were fixed with methanol and stained with 0.01% crystal violet (Beyotime). The number of clones was observed through a microscope (Olympus), and survival fraction was calculated as (number of colonies) / (number of cells seeded) × (plating efficiency).

Flow Cytometry Assay

Annexin V-fluorescein isothiocyanate (FITC)/propidium iodide (PI) Apoptosis Detection Kit (Vazyme) was used for cell apoptosis assay. In brief, 5-8F and SUNE-1 cells with different transfection were seeded into 6-well plates, treated with 0.25% trypsin and washed with precooled phosphate-buffered saline (PBS). Thereafter, cells (2×10^5) were resuspended by 100 μL 1 × binding buffer, followed by staining with 10 μL Annexin V-FITC and 5 μL PI for 10 min without light. Finally, the apoptotic cells were sorted using Attune NxT Flow Cytometer (Invitrogen, Carlsbad, CA, USA).

Western Blot

Western blot analysis was executed in line with previous description (24). The primary antibodies against Cleaved Caspase-3 (Cleaved-cas-3) (ab2302; 1:1000; Abcam, Cambridge, MA. USA), Cleaved Caspase-9 (Cleaved-cas-9) (ab2324; 1:1000; Abcam), extracellular signal-regulated kinases (ERK) (#9102; 1:1000; Cell Signaling Technology; Danvers, MA, USA), phosphor-ERK (p-ERK) (#9101; 1:1000; Cell Signaling Technology), c-Jun N-terminal kinases (JNK) (#9252; 1:1000; Cell Signaling Technology), phosphor-JNK (p-JNK) (#9251; 1:1000; Cell Signaling Technology), GAPDH (ab9485; 1:2500; Abcam) and goat anti-rabbit secondary antibodies

(ab205718; 1:5000; Abcam) were used in this study.

Bioinformatics Analysis and Dual-Luciferase Reporter Assay

The online bioinformatics tool microRNA.org (http://www.microrna.org/microrna/getDownloads.do) was utilized to forecast the potential targets of LINC00114 and specific binding sites.

Dual-luciferase reporter assay was carried out to ensure the association between LINC00114 and miR-203. In brief, the sequences of LINC00114 wild type (WT) containing the binding sites with miR-187-3p and corresponding LINC00114 mutant (MUT) sequences mutated according to its WT sequences were amplified and inserted into the pmirGLO vector (Promega, Madison, WI, USA), named as LINC00114 WT and LINC00114 MUT. Then, LINC00114 WT and LINC00114 MUT were introduced into 5-8F and SUNE-1 cells with miR-187-3p or miR-NC transfection, respectively. After 48 h, the luciferase activity was determined using the Dual-Luciferase Reporter Assay Kit (Promega, Madison, WI, USA) in line with the instruction.

Tumor Formation Assay In Vivo

A total of 20 BALB/c nude mice (male, 6-week-old) were purchased from Beijing HFK Bioscience Co., Ltd. (Beijing, China) and kept in standard growth conditions. Animal experiments obtained the approval of the Animal Care and Use Committee of Urumqi Eye and ENT Specialist Hospital. 5-8F cells were transfected with the sh-LINC00114 or sh-NC. Meanwhile, a part of transfected 5-8F cells was exposed to 4Gy X-ray radiation, divided into sh-LINC00114+4Gy group and sh-NC+4Gy group. Subsequently, stably transfected 5-8F cells were subcutaneously inoculated into the left flank of the groin. After inoculation for one week, the tumor volumes were summarized once a week following the formula: volume (mm^3) = $width^2 \times length \times 0.5$. After 35 days, all mice were killed, and tumor tissues were removed for weighing and other analyses.

Statistical Analysis

Data were processed by SPSS 21.0 (SPSS Inc., Armonk, NY, USA), and exhibited as mean ± standard deviation (SD). The difference between the two groups was performed by Student's *t*-test or among multiple groups by one-way analysis of variance (ANOVA) followed by Tukey's test. Diagnostic value of LINC00114 was estimated by building ROC curves. Overall survival rate was assessed by Kaplan-Meier analysis and log-rank test. Spearman's correlation analysis was utilized to ascertain the correlation between LINC00114 and miR-203 expression. All experiments were repeated at least three times. p-value < 0.05 was regarded as statistically significant.

Results

LINC00114, Aberrantly Upregulated in NPC, was an Independent Diagnostic Marker of NPC

To determine whether LINC00114 was involved in the development of NPC, the expression level of LINC00114 was detected by qRT-PCR. The expression of LINC00114 was significantly increased in serum specimens from NPC patients (n=70) compared with that from healthy subjects (n=50) (Figure 1A). Receiver operating characteristic (ROC) curve was plotted to evaluate the potential diagnostic value of LINC00114 in NPC, and the result showed that the area under ROC curve (AUC) was 0.7894 with 95% confidence interval (CI), ranging from 0.7806 to 0.9353 (Figure 1B). In addition, the expression of LINC00114 in NPC tissues was notably higher than that in adjacent normal tissues (Figure 1C). Additionally, the expression of LINC00114 was prominently enhanced in tumor tissues at TNM stage III and IV relative to tumor tissues at TNM stage I and II (Figure 1D). Besides, the expression of LINC00114 was pronouncedly increased in tumor tissues with distant metastasis compared with that without metastasis (Figure 1E). Moreover, Kaplan-Meier log-rank analysis revealed that the overall survival of NPC patients with high LINC00114 expression was poorer than that with low LINC00114 expression (Figure 1F). These data suggested that dysregulation of LINC00114 was associated with NPC, and LINC00114 could serve as an independent diagnostic and prognostic factor.

LINC00114 was Upregulated in NPC Cell Lines, and its Knockdown Inhibited Cell Proliferation and Migration

To investigate the role of LINC00114 in NPC cells *in vitro*, the endogenous level of LINC00114 was knocked down. Prior to this, we found that the expression of LINC00114 was strengthened in 5-8F and SUNE-1 cells relative to NP69 cells (Figure 2A). Then, the efficiency of LINC00114

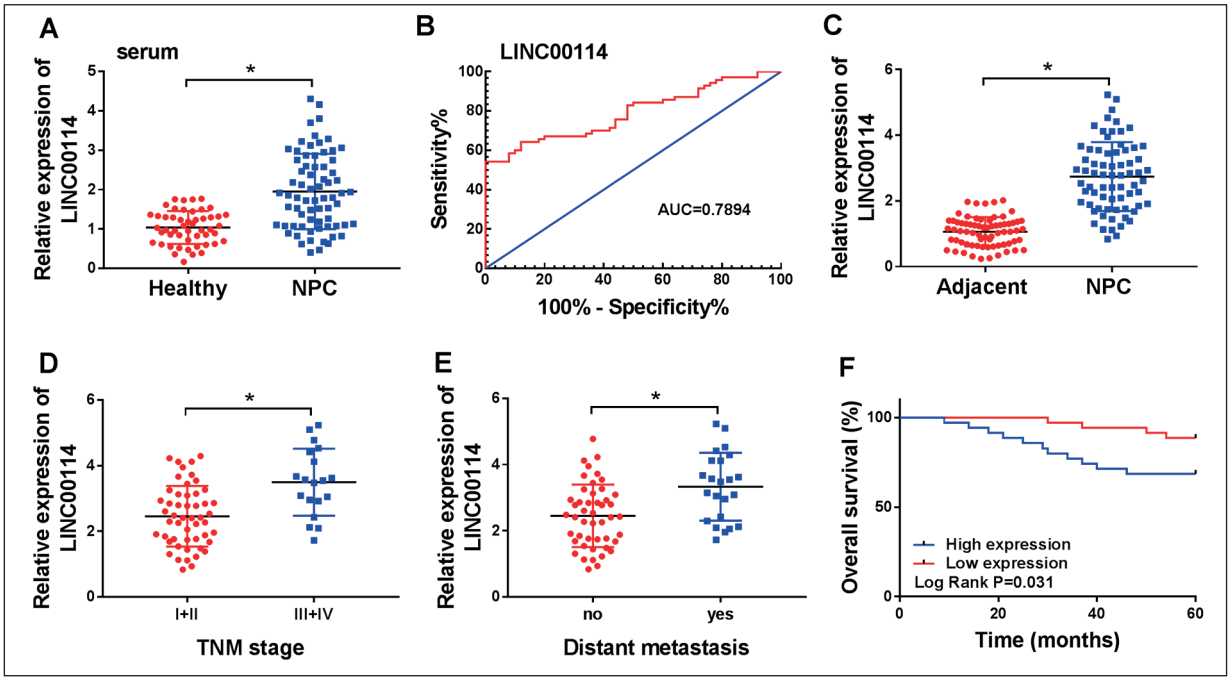

Figure 1. LINC00114 was upregulated in NPC serums and tissues. **A,** The expression of LINC00114 in serums from NPC patients and healthy volunteers was detected by qRT-PCR. **B,** ROC curve was plotted to evaluate the potential diagnostic value of LINC00114. **C,** The expression of LINC00114 in NPC tissues and adjacent normal tissues was detected by qRT-PCR. **D,** The expression of LINC00114 in NPC tissues with different stages was detected by qRT-PCR. **E,** The expression of LINC00114 in NPC tissues with or without distant metastasis was detected by qRT-PCR. **F,** The overall survival within 5 years of NPC patients was analyzed through Kaplan-Meier analysis and log-rank test. *$p < 0.05$.

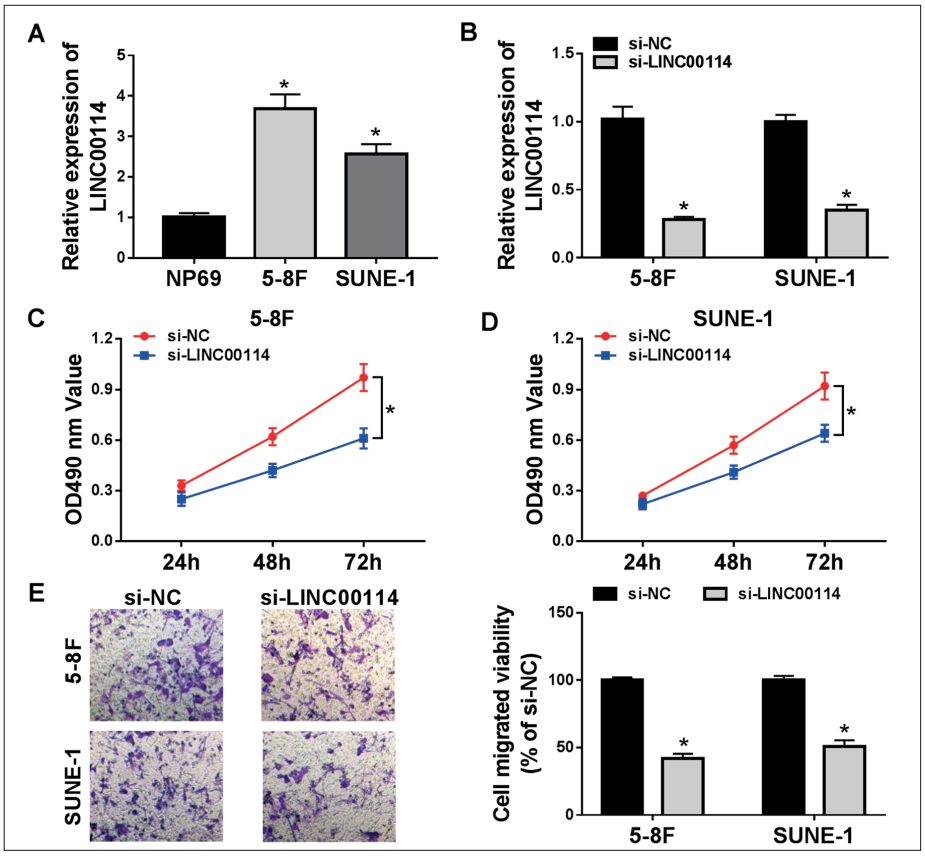

Figure 2. LINC00114 knockdown inhibited proliferation and migration of NPC cells. **A,** The expression of LINC00114 in 5-8F, SUNE-1 and NP69 cells was measured by qRT-PCR. **B,** The efficiency of LINC00114 knockdown in 5-8F and SUNE-1 cells was measured by qRT-PCR. **C-D,** Cell proliferation was monitored by MTT assay. **E,** Cell migration was assessed by transwell assay (100×). *$p < 0.05$.

knockdown was examined, and the result indicated that the LINC00114 expression was significantly decreased in 5-8F and SUNE-1 cells transfected with si-LINC00114 (Figure 2B). Next, MTT assay manifested that the proliferation of 5-8F and SUNE-1 cells was suppressed with the knockdown of LINC00114 (Figure 2C and 2D). Besides, transwell assay concluded that the ability of cell migration was markedly blocked with si-LINC00114 transfection (Figure 2E). The data indicated that LINC00114 knockdown inhibited cell proliferation and migration in NPC.

LINC00114 Knockdown Enhanced the Radiosensitivity of NPC Cells

To monitor the role of LINC00114 on the radiosensitivity, 5-8F and SUNE-1 cells were subjected to radiation at different doses. The survival fractions were compared in 5-8F and SUNE-1 cells transfected with si-LINC00114 or si-NC with the indicated dose of irradiation (0 Gy, 2 Gy, 4 Gy, 6 Gy or 8 Gy) treatment. The result of colony formation experiment presented that the survival fraction was notably suppressed by si-LINC00114 compared with si-NC in a dose-dependent manner (Figure 3A and 3B). Besides, the inhibition rate of cell survival was gradually prominent at 4 Gy groups. Hence, 5-8F and SUNE-1 cells induced with 4 Gy radiation were used for the following experiments. After treatment of 4 Gy radiation, the apoptosis rate of 5-8F and SUNE-1 cells transfected with si-LINC00114 was remarkably elevated compared with si-NC (Figure 3C). Furthermore, the levels of Cleaved-cas-3 and Cleaved-cas-9 detected by western blot were obviously increased in 5-8F and SUNE-1 cells transfected with si-LINC00114 relative to si-NC following the treatment of 4 Gy radiation (Figure 3D). The analyses implied that knockdown of LINC00114 promoted the radiosensitivity of NPC cells.

MiR-203 was Identified as a Target of LINC00114

To explore the underlying action mechanism of LINC00114 in NPC, the putative targets of LINC00114 were predicted and verified. MiR-203 was predicted as a target of LINC00114 by microRNA.org, and there was a specific binding site between miR-203 and LINC00114 (Figure 4A). Then, LINC00114 MUT was mutated based on LINC00114 WT for dual-luciferase reporter assay, and the consequence exhibited that the luciferase activity was remarkably declined in 5-8F and SUNE-1 cells co-transfected with LINC00114 WT and miR-203 relative to miR-NC, while the luciferase activity was unchanged in cells with LINC00114 MUT and miR-203 transfection relative to miR-NC (Figure 4B and 4C). Next, we discovered that miR-203 was significantly down-regulated in 5-8F and SUNE-1 cells compared with that in NP69 cells (Figure 4D). Besides, the expression of miR-203 was enhanced with the knockdown of LINC00114 (Figure 4E). Moreover, the expression of miR-203 was also reduced in NPC tissues (n=70) compared with adjacent normal tissues (n=70) (Figure 4F). Spearman correlation analysis uncovered that miR-203 expression was negatively correlated with LINC00114 expression (Figure 4G). Above data elucidated that LINC00114 targeted miR-203 and regulated its expression.

Inhibition of miR-203 Abolished the Effects of LINC00114 Knockdown on NPC Cells

To further determine the interaction between miR-203 and LINC00114, 5-8F and SUNE-1 cells were introduced with si-LINC00114 and si-LINC00114+anti-miR-203, respectively, si-NC or si-LINC00114+anti-NC as the control. Firstly, the inhibitory efficiency of miR-203 was examined, and the result showed that miR-203 was substantially down-regulated in 5-8F and SUNE-1 cells with anti-miR-203 transfection (Figure 5A). Moreover, the proliferation of 5-8F and SUNE-1 cells, depleted by si-LINC00114 transfection, was obviously recovered by si-LINC00114+anti-miR-203 transfection (Figure 5B and 5C). Besides, the inhibitory metastasis of 5-8F and SUNE-1 cells caused by LINC00114 knockdown was rescued by miR-203 inhibition (Figure 5D). Next, the transfected 5-8F and SUNE-1 cells exposed to radiation were used to monitor the effects of miR-203 inhibition on radiosensitivity. The colony formation assay presented that miR-203 inhibition reinforced the cell survival fraction that was suppressed by LINC00114 knockdown under the treatment of different concentrations of radiation (Figure 5E and 5F). The apoptosis rate was stimulated in 5-8F and SUNE-1 cells with si-LINC00114 transfection but weakened with si-LINC00114+anti-miR-203 transfection (Figure 5G). Additionally, the levels of Cleaved-cas-3 and Cleaved-cas-9 were quantified in radiation-induced 5-8F and

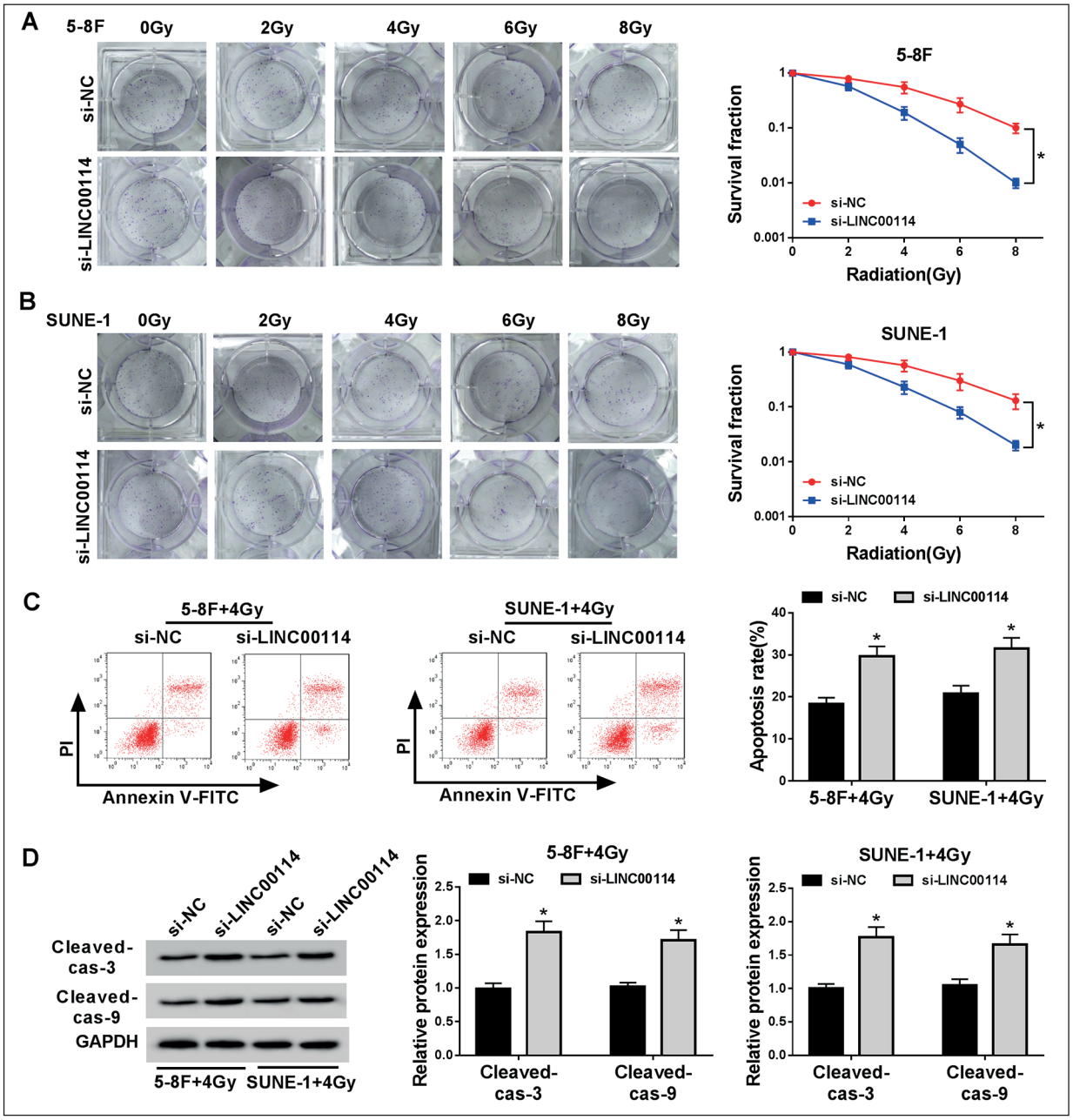

Figure 3. LINC00114 knockdown enhanced radiosensitivity. **A-B,** The cell survival fraction in different doses X-ray treated-5-8F and SUNE-1 cells with si-LINC00114 was investigated by colony formation assay. **C,** Cell apoptosis in 4Gy X-ray-treated-cells was detected by flow cytometry. **D,** The levels of Cleaved-cas-3 and Cleaved-cas-9 were examined by Western blot. *$p < 0.05$.

SUNE-1 cells. The result showed that the expression levels of Cleaved-cas-3 and Cleaved-cas-9 were promoted by LINC00114 knockdown but abolished by miR-203 inhibition (Figure 5H and 5I). Collectively, miR-203 inhibition could reverse the impacts of LINC00114 knockdown on the development and radiosensitivity of NPC cells.

LINC00114 Knockdown Inactivated ERK/JNK Signaling Pathway by Regulating miR-203

To further explore the action mechanism of LINC00114 in NPC, the attention on the signaling pathways was aroused. 5-8F and SUNE-1 cells with si-LINC00114, si-NC, si-LINC00114+anti-miR-203 or si-LINC00114+anti-NC transfection

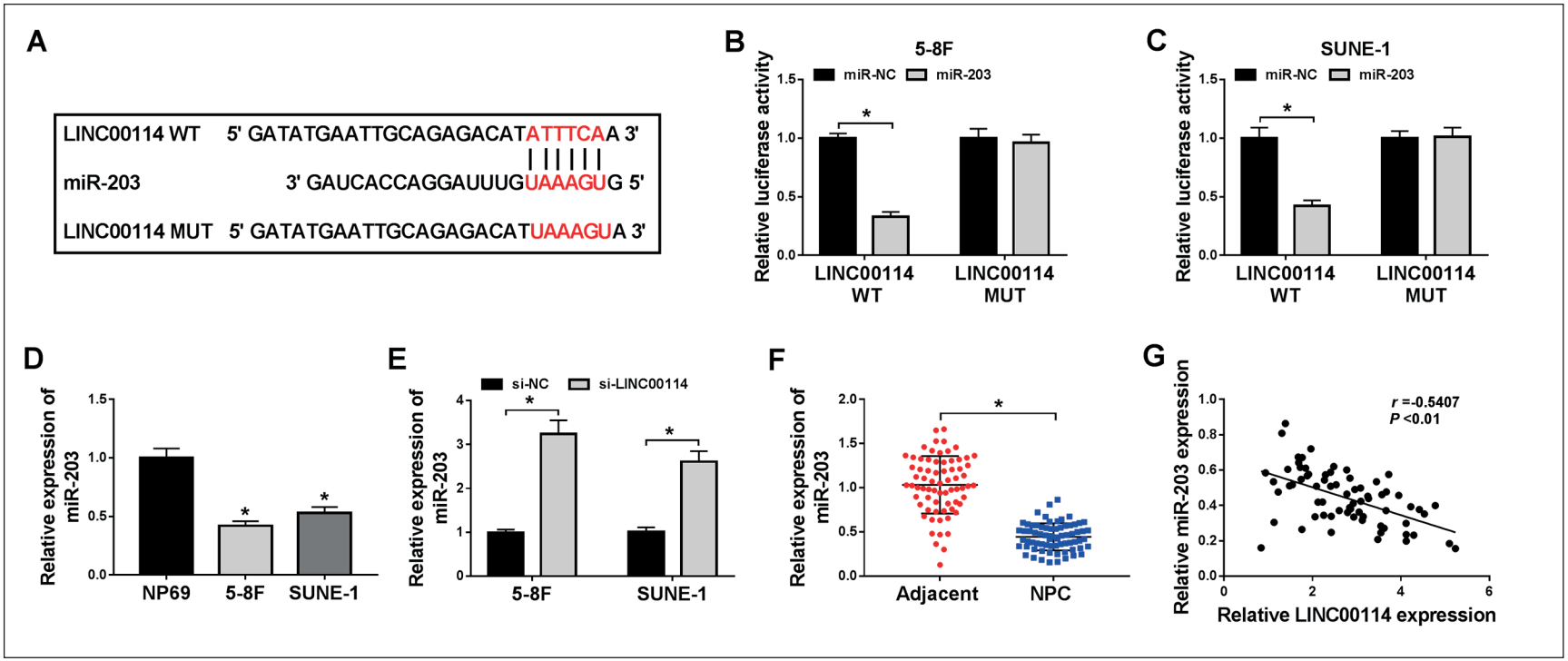

Figure 4. MiR-203 was a target of LINC00114. **A,** The binding sites between LINC00114 and miR-203 were analyzed by bioinformatics too microRNA.org. **B-C,** Dual-luciferase reporter assay was performed to verify the relationship between miR-203 and LINC00114. **D,** The expression of miR-203 in 5-8F, SUNE-1 and NP69 cells was measured by qRT-PCR. **E,** The expression of miR-203 in 5-8F and SUNE-1 cells with si-LINC00114 transfection was measured by qRT-PCR. **F,** The expression of miR-203 in NPC tissues and adjacent normal tissues was measured by qRT-PCR. **G,** The correlation between miR-203 expression and LINC00114 expression was analyzed by Spearman's correlation analyses. *$p < 0.05$.

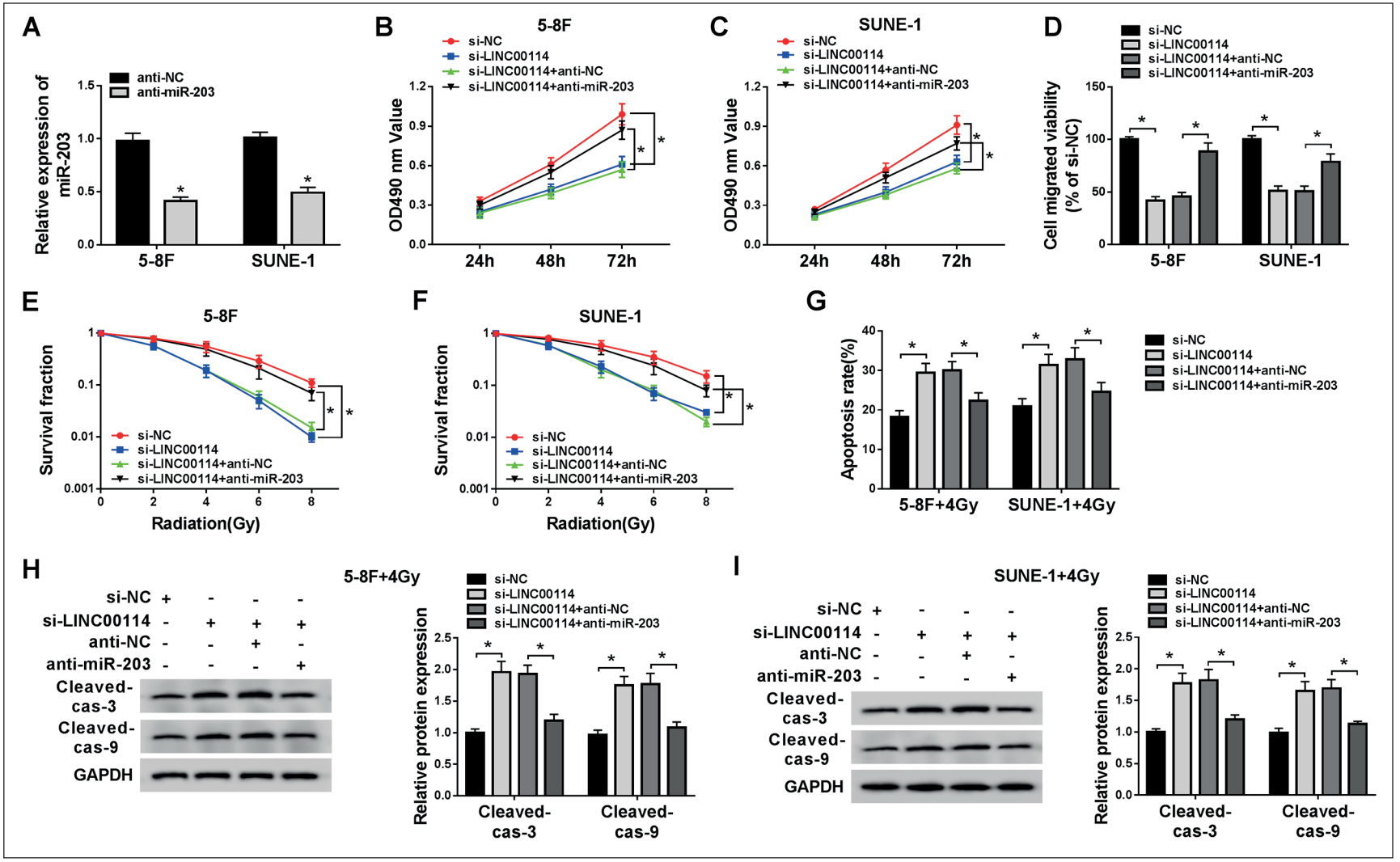

Figure 5. Inhibition of miR-203 reversed the effects of LINC00114 knockdown. 5-8F and SUNE-1 cells were transfected with si-LINC00114 or si-LINC00114+anti-miR-203, si-NC or si-LINC00114+anti-NC as the control. **A,** The efficiency of miR-203 inhibition was detected by qRT-PCR. **B-C,** cell proliferation was determined by MTT assay. **D,** Cell migration was assessed by transwell assay. **E-F,** Cell survival fraction was monitored by colony formation assay. **G,** Cell apoptosis was detected by flow cytometry. **H-I,** The levels of Cleaved-cas-3 and Cleaved-cas-9 were quantified by Western blot. *$p < 0.05$.

were exposed to 4Gy radiation. The analysis of western blot indicated that the levels of p-ERK and p-JNK were inhibited in the si-LINC00114 transfection group relative to the si-NC group. However, the levels of p-ERK and p-JNK were elevated in the si-LINC00114+anti-miR-203 group relative to the si-LINC00114 group in cells with or without radiation treatment (Figure 6A and 6B). The data suggested that LINC00114 knockdown inactivated ERK/JNK pathway through the mediation of miR-203.

LINC00114 Knockdown Impeded Tumor Growth and Radioresistance in Vivo

To ascertain the role of LINC00114 *in vivo*, the tumor formation assay in nude mice was performed. The tumor volume was calculated once a week at 7th day after injection, and the result elucidated that the tumor volume in the sh-LINC00114 group was significantly lower than that in the sh-NC group, and the tumor volume in the sh-LINC00114+4Gy group was notably weaker relative to that in the sh-NC+4Gy group (Figure 7A). After keeping for 35 days, all tumors were removed and weighed. LINC00114 knockdown prominently reduced the tumor weight and strengthened the effects of 4Gy radiation treatment (Figure 7B). Besides, the expression of LINC00114 in tumor tissues with sh-LINC00114 or sh-LINC00114+4Gy injection was significantly declined compared with than in sh-NC or sh-NC+4Gy group (Figure 7C). While the expression of miR-203 in these groups was on the contrary with LINC00114 expression (Figure 7D). Additionally, the levels of p-ERK and p-JNK in tumor tissues were declined with LINC00114 knockdown compared with sh-NC, and the levels of p-ERK and p-JNK were remarkably reduced in the sh-LINC00114+4Gy group compared to that in the sh-NC+4Gy group (Figure 7E). These data testified that LINC00114 knockdown inhibited tumor growth and radioresistance through inactivating ERK/JNK signaling pathway by modulating miR-203.

Discussion

NPC is a more radiosensitive tumor relative to other head and neck tumors, and metastasis is the leading cause in the treatment failure and poor prognosis of NPC[25,26]. Therefore, it is forward-looking to explore novel mechanisms to combat NPC progression and radioresistance. In our exploration, we found LINC00114 expressed with a high level in NPC tissues and cells. LINC00114 knockdown inhibited cell proliferation and migration and promoted radiosensitivity through the impediment of colony formation and the facilitation of cell apoptosis. It was confirmed that miR-203 was a target of linc00114, and miR-203 inhibition could eliminate the effects of LINC00114 knockdown. Besides, ERK/JNK pathway was involved in LINC00114/miR-203 regulatory axis. The role of LINC00114 was also examined in nude mice *in vivo*.

Cancer is a complex disease involving multiple expression changes in a variety of genes, leading to the modulation of cell metastasis, proliferation, cycle, invasion, angiogenesis, radioresistance and chemoresistance. The exploration of ncRNAs provides new insights into the field of cancer and suggests the link between their expression and cancer development[27]. LINC00114, also known as C21orf24[28], is poorly investigated in human cancers. In a previous report, a series of differentially expressed genes were obtained between high- and low-metastasis cells of NPC by microarray expression analysis. ENST00000448579 (gene symbol: LINC00114) was one of these differentially expressed genes with up-regulation. Besides, the validation of qRT-PCR was consistent with the result of microarray[15]. In our study, we quantified the expression level of LINC00114 in NPC. Compared with the serum from healthy volunteers, the expression of LINC00114 was significantly higher in serum from NPC patients. Likewise, the expression of LINC00114 in NPC tumor tissues was notably enhanced than that in adjacent normal tissues. Additionally, we found that advanced NPC had a higher expression of LINC00114 than early NPC. Functional analysis revealed that LINC00114 knockdown suppressed cell proliferation, metastasis and radioresistance *in vitro* and *in vivo*.

Research on miR-203 in cancer has made some progresses. The enrichment of miR-203 weakened the effects of epithelial-mesenchymal transition (EMT) in NPC and maintained the regular phenotype of nasopharyngeal epithelial cells[29]. Besides, a report concluded that JUN, a significantly up-regulated gene in radioresistant NPC, was targeted by miR-203[30]. Qu et al[31] detected a remarkably down-regulated miR-203 from radioresistant NPC cells through microarray analysis and proved that miR-203 mimics reduced the radioresistant of NPC cells *in vivo* and *in vitro*. Consistent with these findings, we also concluded that the expression of miR-203 was reduced in

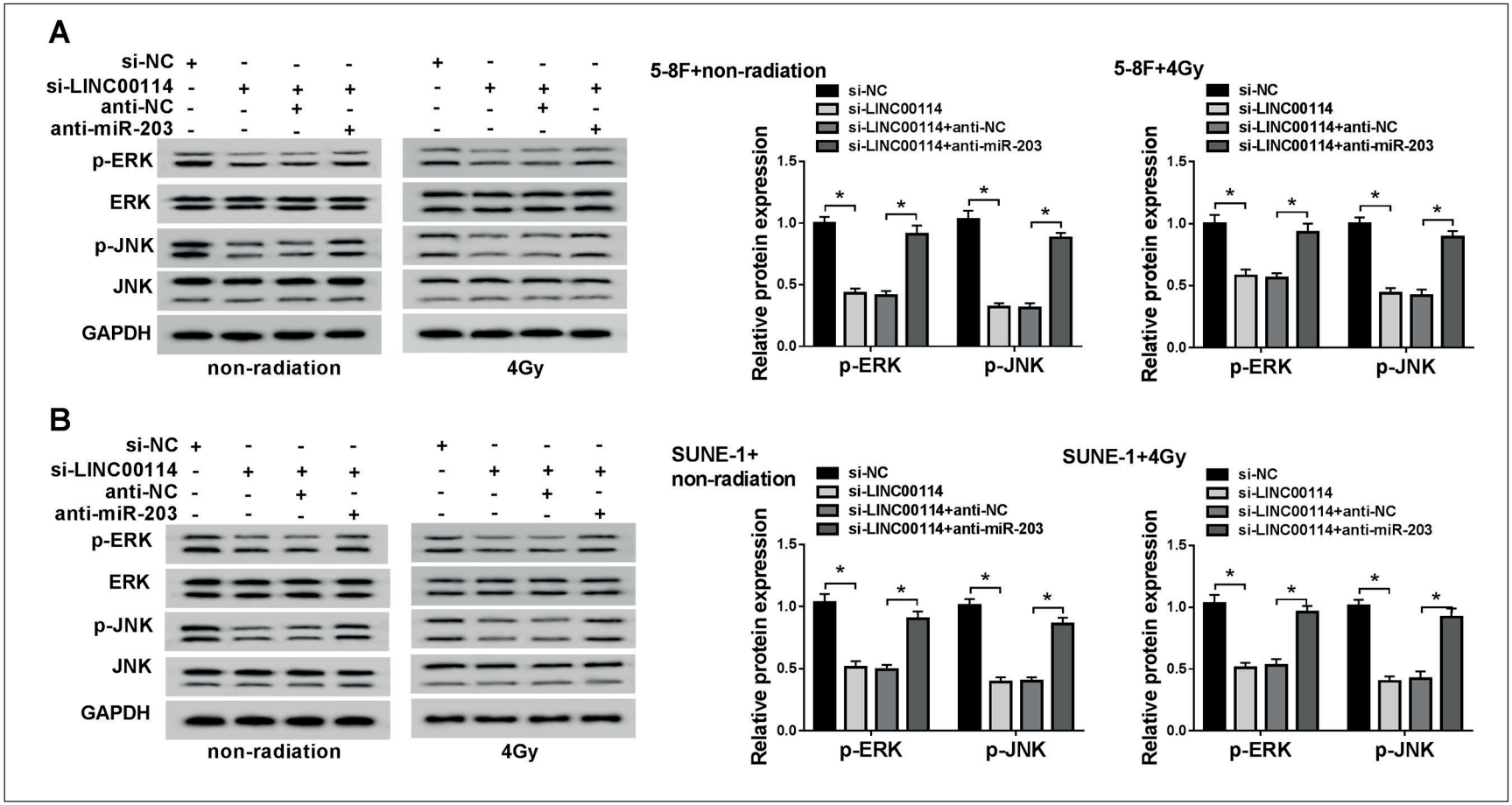

Figure 6. LINC00114 regulated ERK/JNK pathway by targeting miR-203. 5-8F and SUNE-1 cells were transfected with si-LINC00114 or si-LINC00114+anti-miR-203, si-NC or si-LINC00114+anti-NC as the control, and parts of cells were exposed to 4Gy X-ray. **A-B,** The levels of p-ERK and p-JNK were quantified by Western blot. *$p < 0.05$.

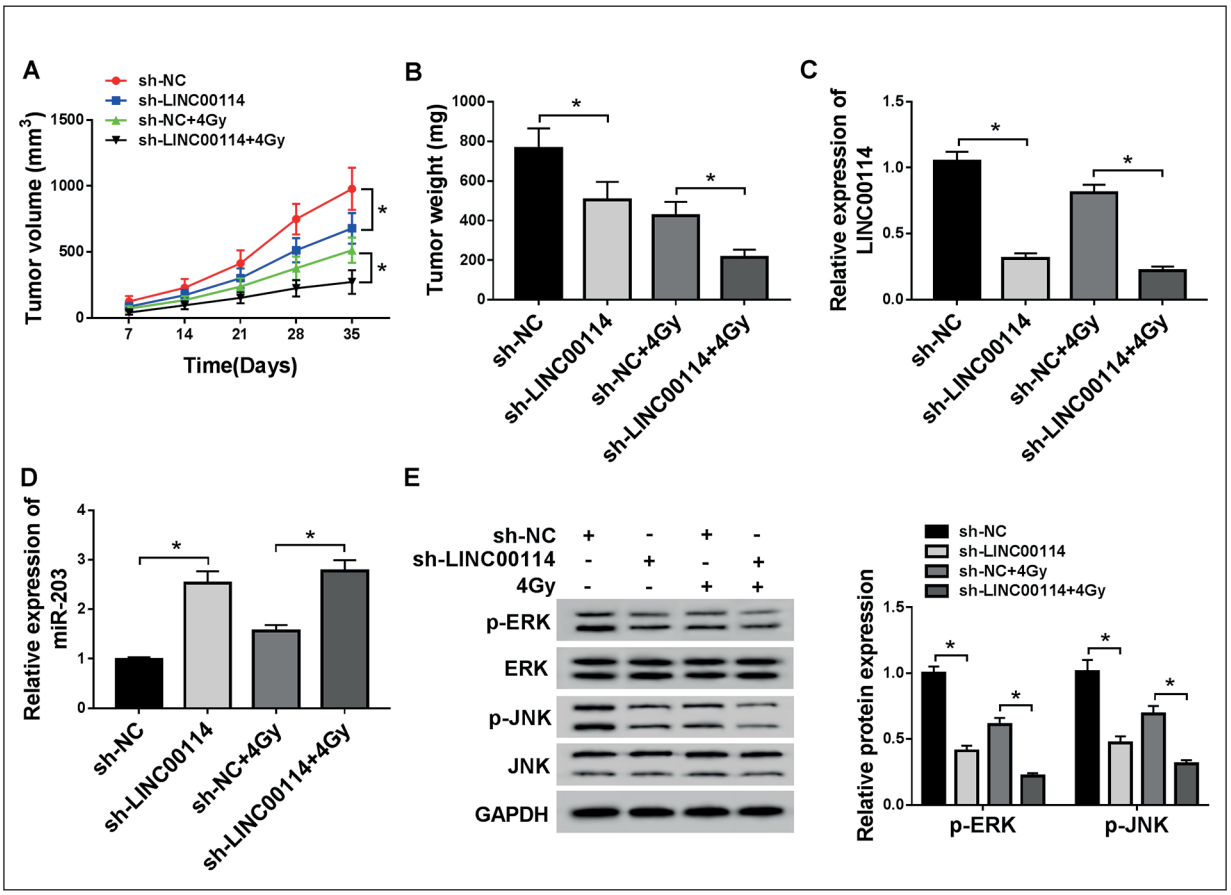

Figure 7. LINC00114 knockdown inhibited tumor growth *in vivo*. **A,** Tumor volume was calculated every 7 days. **B,** Tumor was weighed after injection for 35 days. **C-D,** The expression of LINC00114 and miR-203 in removed tumor tissues was measured by qRT-PCR. **E,** The levels of p-ERK and p-JNK in tumor tissues were detected by Western blot. *$p < 0.05$.

NPC tissues and cells, and miR-203 inhibition reversed the effects of LINC00114 knockdown on NPC progression and radioresistance. These conclusions elucidated that miR-203 played a crucial role in the antagonism of NPC development and radioresistance.

In mammals, the mitogen-activated protein kinases (MAPKs) family contains three well-characterized subfamilies: extracellular signal-regulated kinases (ERK), c-Jun N-terminal kinases (JNK) and p38 kinases[32]. In cancer cells, the activation of MAPKS regulates numerous cellular activities, such as proliferation, differentiation, cell death and survival[33]. Besides, miR-134 was up-regulated in ovarian cancer and contributed to tumor growth and chemosensitivity through the activation of ERK/JNK signaling[34]. Interleukin-33 overexpression was closely linked to poor prognosis of ovarian cancer and accelerated growth and migration of cancer cells through strengthening the phosphorylation of ERK and JNK[35]. Caffeic acid phenethyl ester (CAPE) inhibited cell proliferation and invasion by partly enhancing the expression of ERK and JNK in NPC[36]. These observations showed that the activation of ERK and JNK signaling was closely associated with tumorigenesis and development. In our study, we found LINC00114 knockdown suppressed the phosphorylation of ERK and JNK, while miR-203 inhibition restored this effect, suggesting LINC00114 regulated ERK/JNK signaling pathway by targeting miR-203.

Conclusions

Taken together, LINC00114 was upregulated in NPC and was an independent diagnostic marker. Functional analysis revealed that LINC00114 knockdown suppressed proliferation and migration, increased radiosensitivity *in vitro*, and impeded tumor growth *in vivo*. Mechanism analysis concluded

that LINC00114 contributed to the progression and radioresistance of NPC by activating ERK/JNK signaling pathway *via* targeting miR-203. Our study provided a novel theoretical basis for NPC treatment and antagonism to radioresistance.

Conflict of Interest

The Authors declare that they have no conflict of interests.

Funding

This work approved by Natural Science Foundation of Xinjiang Uygur Autonomous Region (No. 2017D01A19).

References

1) Song Y, Yang J, Bai WL, Ji WY. Antitumor and immunoregulatory effects of astragalus on nasopharyngeal carcinoma in vivo and in vitro. Phytother Res 2011; 25: 909-915.
2) Orr RD, Salo PT. Atlantoaxial instability complicating radiation therapy for recurrent nasopharyngeal carcinoma. A case report. Spine (Phila Pa 1976) 1998; 23: 1280-1282.
3) Sun X, Tong LP, Wang YT, Wu YX, Sheng HS, Lu LJ, Wang W. Can global variation of nasopharynx cancer be retrieved from the combined analyses of IARC Cancer Information (CIN) databases? PLoS One 2011; 6: e22039.
4) Wei WI, Sham JS. Nasopharyngeal carcinoma. Lancet 2005; 365: 2041-2054.
5) Wang H, Chen H, Zhou H, Yu W, Lu Z. Cyclin-dependent kinase inhibitor 3 promotes cancer cell proliferation and tumorigenesis in nasopharyngeal carcinoma by targeting p27. Oncol Res 2017; 25: 1431-1440.
6) Hu CM, Zhang L. Nanoparticle-based combination therapy toward overcoming drug resistance in cancer. Biochem Pharmacol 2012; 83: 1104-1111.
7) Erkal HS, Serin M, Cakmak A. Nasopharyngeal carcinomas: analysis of patient, tumor and treatment characteristics determining outcome. Radiother Oncol 2001; 61: 247-256.
8) Lee AWM, Ng WT, Chan JYW, Corry J, Mäkitie A, Mendenhall WM, Rinaldo A, Rodrigo JP, Saba NF, Strojan P, Suárez C, Vermorken JB, Yom SS, Ferlito A. Management of locally recurrent nasopharyngeal carcinoma. Cancer Treat Rev 2019; 79: 101890.
9) Bensouda Y, Kaikani W, Ahbeddou N, Rahhali R, Jabri M, Mrabti H, Boussen H, Errihani H. Treatment for metastatic nasopharyngeal carcinoma. Eur Ann Otorhinolaryngol Head Neck Dis 2011; 128: 79-85.
10) Mercer TR, Dinger ME, Mattick JS. Long non-coding RNAs: insights into functions. Nat Rev Genet 2009; 10: 155-159.
11) Lian Y, Xiong F, Yang L, Bo H, Gong Z, Wang Y, Wei F, Tang Y, Li X, Liao Q, Wang H, Zhou M, Xiang B, Wu X, Li Y, Li X, Chen X, Li G, Guo C, Zeng Z, Xiong W. Long noncoding RNA AFAP1-AS1 acts as a competing endogenous RNA of miR-423-5p to facilitate nasopharyngeal carcinoma metastasis through regulating the Rho/Rac pathway. J Exp Clin Cancer Res 2018; 37: 253.
12) Wen X, Liu X, Mao YP, Yang XJ, Wang YQ, Zhang PP, Lei Y, Hong XH, He QM, Ma J, Liu N, Li YQ. Long non-coding RNA DANCR stabilizes HIF-1alpha and promotes metastasis by interacting with NF90/NF45 complex in nasopharyngeal carcinoma. Theranostics 2018; 8: 5676-5689.
13) Zheng ZQ, Li ZX, Zhou GQ, Lin L, Zhang LL, Lv JW, Huang XD, Liu RQ, Chen F, He XJ, Kou J, Zhang J, Wen X, Li YQ, Ma J, Liu N, Sun Y. Long noncoding RNA FAM225A promotes nasopharyngeal carcinoma tumorigenesis and metastasis by acting as ceRNA to sponge miR-590-3p/miR-1275 and upregulate ITGB3. Cancer Res 2019; 79: 4612-4626.
14) Fan C, Wei Q, Hao Z, Li G. Prediction and functional analysis of lincRNAs targeted by miRNAs. Yi Chuan 2014; 36: 1226-1234.
15) Wen X, Tang X, Li Y, Ren X, He Q, Yang X, Zhang J, Wang Y, Ma J, Liu N. Microarray expression profiling of long non-coding RNAs involved in nasopharyngeal carcinoma metastasis. Int J Mol Sci 2016; 17(11). pii: E1956.
16) Tseng KC, Chiang-Hsieh YF, Pai H, Chow CN, Lee SC, Zheng HQ, Kuo PL, Li GZ, Hung YC, Lin NS, Chang WC. microRPM: a microRNA prediction model based only on plant small RNA sequencing data. Bioinformatics 2018; 34: 1108-1115.
17) Pu M, Chen J, Tao Z, Miao L, Qi X, Wang Y, Ren J. Regulatory network of miRNA on its target: coordination between transcriptional and post-transcriptional regulation of gene expression. Cell Mol Life Sci 2019; 76: 441-451.
18) Lin C, Zong J, Lin W, Wang M, Xu Y, Zhou R, Lin S, Guo Q, Chen H, Ye Y, Zhang B, Pan J. EBV-miR-BART8-3p induces epithelial-mesenchymal transition and promotes metastasis of nasopharyngeal carcinoma cells through activating NF-kappaB and Erk1/2 pathways. J Exp Clin Cancer Res 2018; 37: 283.
19) Lu J, Liu QH, Wang F, Tan JJ, Deng YQ, Peng XH, Liu X, Zhang B, Xu X, Li XP. Exosomal miR-9 inhibits angiogenesis by targeting MDK and regulating PDK/AKT pathway in nasopharyngeal carcinoma. J Exp Clin Cancer Res 2018; 37: 147.
20) Liang TS, Zheng YJ, Wang J, Zhao JY, Yang DK, Liu ZS. MicroRNA-506 inhibits tumor growth and metastasis in nasopharyngeal carcinoma through the inactivation of the Wnt/beta-catenin signaling pathway by down-regulating LHX2. J Exp Clin Cancer Res 2019; 38: 97.
21) Wang B, Li X, Zhao G, Yan H, Dong P, Watari H, Sims M, Li W, Pfeffer LM, Guo Y, Yue J. miR-203 inhibits ovarian tumor metastasis by targeting BIRC5

and attenuating the TGFbeta pathway. J Exp Clin Cancer Res 2018; 37: 235.

22) Xiang J, Bian C, Wang H, Huang S, Wu D. MiR-203 down-regulates Rap1A and suppresses cell proliferation, adhesion and invasion in prostate cancer. J Exp Clin Cancer Res 2015; 34: 8.

23) Taipaleenmäki H, Browne G, Akech J, Zustin J, van Wijnen AJ, Stein JL, Hesse E, Stein GS, Lian JB. Targeting of Runx2 by miR-135 and miR-203 impairs progression of breast cancer and metastatic bone disease. Cancer Res 2015; 75: 1433-1444.

24) Li W, Wu X, She W. LncRNA POU3F3 promotes cancer cell migration and invasion in nasopharyngeal carcinoma by up-regulating TGF-beta1. Biosci Rep 2019; 39(1). pii: BSR20181632.

25) Lin JC, Jan JS, Hsu CY. Pilot study of concurrent chemotherapy and radiotherapy for stage IV nasopharyngeal cancer. Am J Clin Oncol 1997; 20: 6-10.

26) Yang Q, Zhang MX, Zou X, Liu YP, You R, Yu T, Jiang R, Zhang YN, Cao JY, Hong MH, Liu Q, Guo L, Kang TB, Zhu XF, Chen MY. A prognostic bio-model based on SQSTM1 and N-Stage identifies nasopharyngeal carcinoma patients at high risk of metastasis for additional induction chemotherapy. Clin Cancer Res 2018; 24: 648-658.

27) Tano K, Akimitsu N. Long non-coding RNAs in cancer progression. Front Genet 2012; 3: 219.

28) Caracausi M, Rigon V, Piovesan A, Strippoli P, Vitale L, Pelleri MC. A quantitative transcriptome reference map of the normal human hippocampus. Hippocampus 2016; 26: 13-26.

29) Zuo LL, Zhang J, Liu LZ, Zhou Q, Du SJ, Xin SY, Ning ZP, Yang J, Yu HB, Yue WX, Wang J, Zhu FX, Li GY, Lu JH. Cadherin 6 is activated by Epstein-Barr virus LMP1 to mediate EMT and metastasis as an interplay node of multiple pathways in nasopharyngeal carcinoma. Oncogenesis 2017; 6: 402.

30) Guo Y, Zhang Y, Zhang SJ, Ma YN, He Y. Comprehensive analysis of key genes and microRNAs in radioresistant nasopharyngeal carcinoma. BMC Med Genomics 2019; 12: 73.

31) Qu JQ, Yi HM, Ye X, Zhu JF, Yi H, Li LN, Xiao T, Yuan L, Li JY, Wang YY, Feng J, He QY, Lu SS, Xiao ZQ. MiRNA-203 reduces nasopharyngeal carcinoma radioresistance by targeting IL8/AKT signaling. Mol Cancer Ther 2015; 14: 2653-2664.

32) Cargnello M, Roux PP. Activation and function of the MAPKs and their substrates, the MAPK-activated protein kinases. Microbiol Mol Biol Rev 2011; 75: 50-83.

33) Raman M, Chen W, Cobb MH. Differential regulation and properties of MAPKs. Oncogene 2007; 26: 3100-3112.

34) Wu J, Sun Y, Zhang PY, Qian M, Zhang H, Chen X, Ma D, Xu Y, Chen X, Tang KF. The Fra-1-miR-134-SDS22 feedback loop amplifies ERK/JNK signaling and reduces chemosensitivity in ovarian cancer cells. Cell Death Dis 2016; 7: e2384.

35) Tong X, Barbour M, Hou K, Gao C, Cao S, Zheng J, Zhao Y, Mu R, Jiang HR. Interleukin-33 predicts poor prognosis and promotes ovarian cancer cell growth and metastasis through regulating ERK and JNK signaling pathways. Mol Oncol 2016; 10: 113-125.

36) Chiang KC, Yang SW, Chang KP, Feng TH, Chang KS, Tsui KH, Shin YS, Chen CC, Chao M, Juang HH. Caffeic acid phenethyl ester induces n-myc downstream regulated gene 1 to inhibit cell proliferation and invasion of human nasopharyngeal cancer cells. Int J Mol Sci 2018; 19. pii: E1397.